Using LISA-like gravitational wave detectors to search for primordial black holes

Huai-Ke Guo, Jing Shu, and Yue Zhao

Phys. Rev. D **99**, 023001 — Published 2 January 2019

DOI: 10.1103/PhysRevD.99.023001

Using LISA-like Gravitational Wave Detectors to Search for Primordial Black Holes

Huai-Ke Guo,[1] Jing Shu,[1,2,3] and Yue Zhao[4,5]

[1] *CAS Key Laboratory of Theoretical Physics, Institute of Theoretical Physics, Chinese Academy of Sciences, Beijing 100190, China*
[2] *School of Physical Sciences, University of Chinese Academy of Sciences, Beijing 100149, P. R. China*
[3] *CAS Center for Excellence in Particle Physics, Beijing 100049, China*
[4] *Tsung-Dao Lee Institute, and Department of Physics and Astronomy, Shanghai Jiao Tong University, Shanghai 200240*
[5] *Michigan Center for Theoretical Physics, University of Michigan, Ann Arbor, MI 48109*

Primordial black holes (PBHs), which could be naturally produced in the early universe, remain a promising dark matter candidate. They can merge with a supermassive black hole (SMBH) at the center of a galaxy and generate a gravitational wave (GW) signal in the favored frequency region of laser interferometer space antenna (LISA)-like experiments. In this study, we investigated the event rate calculation for extreme mass ratio inspirals and the sensitivities of various proposed GW detectors. We determined that such experiments offer a novel and effective tool for testing scenario where PBHs constitute (a fraction of) dark matter. The PBH energy density fraction of DM ($f_{\rm PBH}$) can potentially be explored for values as small as $10^{-3} - 10^{-4}$. Further the LISA can search for PBH masses up to $10^{-2} - 10^{-1} M_\odot$. Other proposed GW experiments can investigate lower PBH mass regimes.

Introduction. Dark matter (DM) constitutes approximately 27% of the energy density in the current universe [1]. However the identity of DM remains a mystery. Although a favored candidate is any new particle beyond the Standard Model, other alternative candidates remain possible. One intriguing possibility is primordial black holes (PBH) [2] (for a PBH review, see e.g., [3]), which has been intensively studied in the past 50 years because of its substantial impact on fundamental physics, the early universe, and cosmology. Additionally much effort has been expended to study PBH as DM experimentally by using gravitational lensing [4–12], the cosmic microwave background temperature anisotropies and polarizations [13, 14]. The validity as well as astrophysical uncertainties of some constraints remain the subject of debate [15, 16], and other aspects of independent measurements on this debate would be valuable.

Gravitational wave (GW) events from the merging of black hole binaries and detected by the Laser Interferometer Gravitational-Wave Observatory (LIGO) and Virgo collaborations [17–19] have ushered in the era of GW astronomy, which provides a new avenue for studying PBHs. Immediately after this breakthrough, Refs. [2, 20–28] have investigated whether the source of the GW signals detected by LIGO could be PBHs comprising a nontrivial proportion of DM [79]. Theoretically, this is topical and innovative. However we may never know whether these $\mathcal{O}(10)$ $M_\odot$ black holes (BHs) detected by the LIGO and Virgo collaboration are PBHs or stellar BHs. Additionally, we may never ascertain the PBH densities, whose possible densities may vary considerably. This is because the LIGO is not suitable for probing other PBH mass ranges regardless of whether they were caused by shifted frequency regions or reduced magnitude of GW radiation.

Recently, the Laser Interferometer Space Antenna (LISA), which targets a much lower frequency regime, was approved [29]. One major scientific goal of the LISA is to measure GWs produced by the merger of a supermassive BH (SMBH) and a compact object (CO), such as a neutron star, white dwarf, or BH. Such mergers are referred to as extreme mass ratio inspirals(EMRIs). In EMRIs [30], GW frequencies are mainly determined by SMBH mass, independent of CO mass. In contrast to the more limited scope of the LIGO, we could potentially access a vast mass range of PBHs, lying outside the mass window of astrophysical COs. Observing such events may lead to the discovery of PBHs. Moreover, the DM profile peaks at the center of a galaxy, indicating a high number density of PBHs near an SMBH serving as the DM candidate. This may induce a considerable EMRI rate caused by PBH-SMBH mergers, and allow the PBH densities to be ascertained.

Motivated by aforementioned considerations, we performed the first solid study on event rate estimation for PBH-SMBH mergers for different LISA-like experiments. The event rate is calculated by combining the PBH-DM halo profile, GW strain and detection, and the intrinsic EMRI rate for a PBH-SMBH, where the last element is critical because it rescales CO masses on the basis of the SMBH-stellar BH EMRI rate from numerical simulations. By combining all the results, we obtained the first expected sensitivity curve of the PBH energy density fraction of DM ($f_{\rm PBH}$) for different LISA-like experiments, which represents a strong physics motivation for conducting experiments to seek PBHs. Our results indicate that not only could sensitivity to $f_{\rm PBH}$ reach $10^{-3} - 10^{-4}$, which is superior to the sensitivity of gravitational lensing, but also could the probed PBH masses be smaller than the astrophysical CO mass window, which provides opportunities for PBH discovery.

Components of EMRI Rate Calculation. EMRI has been thoroughly studied in the context of astrophysics. The event rate observed using a GW detector can be

written as,

$$\Gamma = \int \mathcal{R}(M,\mu)\left(\frac{dn(M,z)}{dM}dM\right)(p(s,z)ds)\left(\frac{dV_c}{dz}dz\right). \quad (1)$$

$\mathcal{R}(M,\mu)$ is the intrinsic EMRI rate in a galaxy hosting a SMBH with mass M. The mass of the CO is μ. $dn(M,z)/dM$ and $p(s,z)$ are the mass spectrum and spin s distribution of the SMBHs, respectively. We can remove the redshift z-dependence since we late times are our only concern. According to the popIII model [31], most of the SMBHs in the LISA range (i.e., $M \leq 10^7\ M_\odot$) are expected to have near maximal spins. Furthermore, different spin distributions change the EMRI rates by less than 10% [32]. Thus, we simply set $s = 0.999$. $\left(\frac{dV_c}{dz}dz\right)$ is the comoving volume integral. The sensitivity of an experiment imposes a maximum z, z_{max}, as a function of (M, s, μ).

In subsequent sections, we describe the components necessary for calculating Eq.(1). Subsequently we combine these components to ascertain the event rates for various GW detectors.

DM Halo Profile. EMRIs are mainly produced by COs within the radius of influence of an SMBH [33],

$$r_h = \frac{GM}{\sigma^2} = 2\text{pc}\left(\frac{M}{3\times10^6 M_\odot}\right)^{1/2}. \quad (2)$$

In the preceding equation, σ is the velocity dispersion in the bulge that is related to M [34–36]. Because r_h is $\mathcal{O}$(pc), the EMRI rate is sensitive to the DM energy density in the innermost region. Although collisionless cold DM demonstrates a cuspy profile [37–40], a cored profile may be obtained if other effects, such as baryonic feedback, are included [41]. Furthermore, under the assumption of adiabatic growth of SMBHs, a spike can be induced [42, 43] and is more pronounced for a Kerr SMBH [44]. Ref. [25] studied the PBH-PBH merger rate in the case of a spike connected to the Navarro-Frenk-White(NFW) profile.

In this letter, we use a vanilla NFW profile [38, 39]; cored (spiky) profiles lead to smaller (larger) PBH-PBH merger. The NFW profile can be parametrized as

$$\rho(r) = \frac{\rho_s}{\frac{r}{R_s}(1+\frac{r}{R_s})^2}, \quad (3)$$

where ρ_s and R_s are the characteristic density and scale radius, respectively. The enclosed mass within a radius R is $4\pi\rho_s R_s^3 g(c)$, where $c = R/R_s$ and $g(x) = \ln(1+x) - x/(1+x)$. A cutoff radius is conventionally defined such that the enclosed average DM energy density is 200 times the critical density of the universe ρ_c, yielding

$$\rho_s = \frac{200}{3}\frac{c_{200}^3}{g(c_{200})}\rho_c; \quad R_s = \left[\frac{M_{200}}{4\pi\rho_s g(c_{200})}\right]^{1/3}. \quad (4)$$

At small redshift, the concentration-mass relation [45] indicates

$$c_{200} = 10^{0.905}\left(\frac{M_{200}}{10^{12}h^{-1}M_\odot}\right)^{-0.101}. \quad (5)$$

Here, $h = 0.677$ is the Hubble parameter measured by Plank. Because Eq. (5) holds only at a small z, we truncate our calculation at a maximal distance, $z \leq 1$ ($r_0 \leq 3.5$Gpc).

Finally, M_{200} and M can be related as [46],

$$\frac{M}{3\times10^6 M_\odot} \approx 3.3\left(\frac{M_{200}}{10^{12}M_\odot}\right)^{1.65}. \quad (6)$$

Therefore, the DM halo profile can be expressed as a simple function of the SMBH mass. Accordingly, the total DM mass within r_h is approximately 10^{-2} the SMBH mass, which is a small perturbation.

Here we want to emphasize that the number of PBHs with mass larger than $\mathcal{O}(1M_\odot)$ in galaxies with lighter SMBHs may be smaller than one within r_h. In this case, one should take our estimation based on NFW profile in a statistical manner. When estimating event rate, we will perform the integration on many galaxies. In the parameter region of interest, the PBH number is never too small in a galaxy. This makes our estimation based on NFW profile remain solid

Gravitational Wave Strain and Signal-to-Noise Ratio. Modeling GW emission from an EMRI system is nontrivial. Several formalisms have been studied. The analytic kludge (AK) model [47, 48] is computationally less expensive than the numerical kludge model [49, 50]. Within the AK formalism, the two approximations are labeled AKK and AKS, which give optimistic and conservative estimates of the SNR, characterizing the uncertainties. GW emission can be estimated for circular and equatorial EMRIs by using the Teukolsky equation [51–53], which was used in [54] to estimate the EMRI rate for the LISA. The obtained result consistently falls between those from AKK and AKS [32]; even the orbits of the EMRIs generically exhibit moderate eccentricity and are inclined. Moreover, the results obtained by using three methods are very close to each other for smaller SMBHs [32], as we illustrate in a subsequent section, and provide the predominate event rates. Therefore, we employ the circular orbit approximation to calculate GW radiation emission.

The characteristic strain for harmonics m is [53],

$$h_{c,1} = \frac{5}{\sqrt{672\pi}}\frac{\eta^{1/2}M}{r_o}\tilde{\Omega}^{1/6}\mathcal{H}_{c,1}\ ,$$
$$h_{c,m} = \sqrt{\frac{5(m+1)(m+2)(2m+1)!m^{2m}}{12\pi(m-1)[2^m m!(2m+1)!!]^2}}\frac{\eta^{1/2}M}{r_o} \times\tilde{\Omega}^{(2m-5)/6}\mathcal{H}_{c,m}, \quad m \geq 2\ . \quad (7)$$

Here, $\eta = \mu/M$ and r_o is the distance to Earth, the dimensionless orbital angular velocity $\tilde{\Omega} \equiv M\Omega = 1/(\tilde{r}^{3/2}+s)$ determines the GW frequency f, where $\tilde{r} \equiv r/M$ with r as the Boyer-Lindquist radial coordinates of the orbit. $\mathcal{H}_{c,m}$ is the relativistic correction [53].

The maximal frequency $f_{\max}$ occurs at the innermost stable circular orbit (ISCO) at radius $r_{\rm ISCO}$, which is a

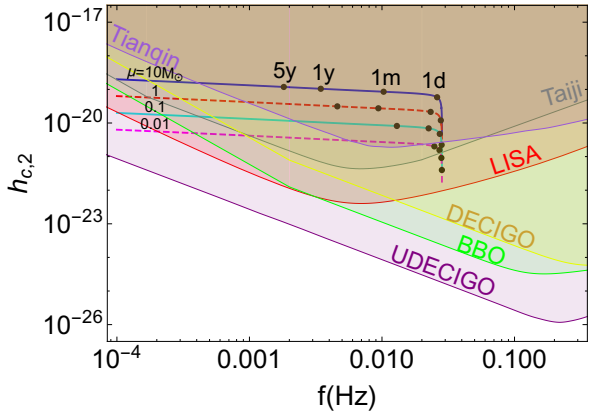

FIG. 1: Characteristic strain $h_{c,2}$ is plotted for different PBH mass μ selections. The SMBH has a mass and spin of $10^6 M_\odot$ and 0.999, respectively. The distance to Earth is taken to be 1Gpc. The dots indicate the remaining time before the merger. The sensitivities of various proposed experiments, $h_n(f)$, are also presented.

function of M and a [55]. In Fig. 1, we present $h_{c,2}$ with different choices of μ. The experimental sensitivity is quantified by $h_n(f_m) \equiv \sqrt{f S_n(f_m)}$, where $S_n(f_m)$ is the one-sided noise power spectral density [56]. The detectors include the LISA with the optimistic configuration(C1) [57], the Taiji [58] and TianQin [59] programs, Big Bang Observer (BBO), DECi-hertz Interferometer Gravitational wave Observatory (DECIGO) and Ultimate-DECIGO(UDECIGO) [60] [80].

A qualitative comparison between the LISA and LIGO is enlightening. Although the LISA and LIGO exhibit their optimal sensitivities at different frequency regimes, the h_n values of the LISA and LIGO are comparable. At approximately $r_{\rm ISCO}$, h_c scales as $\sqrt{\mu M}$. The events using the LIGO have masses of $\mathcal{O}(10)\ M_\odot$. At the same distance, a similar order of magnitude of h_c can be achieved if μ is approximately $10^{-3} M_\odot$ when M is approximately $10^6 M_\odot$. This indicates that LISA-like GW detectors have potential to probe light PBHs.

A GW signal can be detected only when the SNR exceeds a certain threshold. The SNR can be calculated as

$$\mathrm{SNR}^2 = \frac{\mathcal{S}^2}{\mathcal{N}^2} = \sum_m \int \left[\frac{h_{c,m}(f_m)}{h_n(f_m)}\right]^2 d\ln f_m, \qquad (8)$$

where $\mathcal{S}$ and $\mathcal{N}$ are the signal and noise, respectively, obtained though matched filtering [56]. A widely adopted threshold is SNR ≥ 15.

Although slow inspirals may be long-lasting (e.g., $\mathcal{O}$(Gyr)). LISA-like GW detectors can only operate at timescales of $\mathcal{O}$(yr). The GW frequency achieves its maximal value f_{max} when r is approximately $r_{\rm ISCO}$, after which the inspiral stops and the plunge occurs. Only a finite frequency window near the maximal frequency can be recorded during the operation of an experiment. A truncation must accordingly be imposed in Eq.(8). The total time remaining before the plunge is [53, 61]

$$T = \frac{5}{256}\frac{1}{\mu}\frac{M^2}{\tilde{\Omega}^{8/3}}\mathcal{T}, \qquad (9)$$

where $\mathcal{T}$ is the general relativistic correction [53]. Setting T to the operating time yields f_{min}.

For light PBHs, the frequency variation can be tiny on timescales of $\mathcal{O}$(yr). Within this limit, $\Delta f/f \sim \mu/M^2$. For a fixed μ, a smaller M provides a larger integral range during the calculation of SNR. For each EMRI, the SNR imposes an upper limit on redshift. Thus, the limit of the spatial integral is set as $z_{\rm max} = min(z|_{\rm SNR=15}, 1)$.

Intrinsic EMRI Rate for PBH-SMBH. The intrinsic EMRI rate can be calculated by solving the Fokker-Planck equation, which describes the diffusion of CO distribution functions. This Fokker-Planck equation can be conveniently written in a dimensionless form [62], and this procedure is an efficient method for studying the EMRI intrinsic rate of arbitrary masses. Therefore, the results for standard EMRIs can be extrapolated due to the bigger range of masses for many of the PBHs. Here we follow [63] and present an analytical formula to scale $\mathcal{R}$ for stellar BHs on the basis of PBH properties.

The SMBH-stellar BH intrinsic EMRI rate has been studied in [62, 64, 65]. The mass and number density of stellar BHs are taken, respectively, as $10M_\odot$ and 0.1% of an astrophysical object's number density within r_h, therefore, the number density of PBH is related to the SMBH mass as [62]

$$n_{\rm BH} = 40\ {\rm pc}^{-3}\left(\frac{M}{3\times10^6 M_\odot}\right)^{-1/2}. \qquad (10)$$

The intrinsic EMRI rate scales with respect to M as [54, 62]

$$\mathcal{R}_{\rm astro}(M) = 400{\rm Gyr}^{-1}\left(\frac{M}{3\times10^6 M_\odot}\right)^{-0.15}. \qquad (11)$$

Subsequently, we study how Eq.(11) scales as a function of PBH number density and mass.

First, rescaling the PBH number density with respect to that of stellar BHs is straightforward,

$$\mathcal{G}(M,\mu) = f_{\rm PBH}\frac{\rho_{\rm NFW}(M, r_h(M))/\mu}{n_{\rm BH}(M)}. \qquad (12)$$

When $\mu = 10M_\odot$ and $M = 10^6 M_\odot$, $\mathcal{G}$ is $\mathcal{O}(1)$.

A CO changes its orbit through one of two processes: *i*) gravitational scattering with another CO object; *ii*) energy loss through GW radiation. If an SMBH-CO merger is induced by GW radiation after many orbits, a slow inspiral results. For a slow inspiral to be detected using GW detectors, the orbit of the slow inspirals should not be disrupted by gravitational scattering, which is simply a redistribution in the phase space. Competition between the times scales associated with *i*) and *ii*) can be used to set the criteria for a detectable EMRI [81].

The time scale associated with the scattering of a PBH to the orbit of a slow inspiral is a function of relaxation time t_h at r_h. The relaxation time is determined by the species with the largest $m_i^2 n_i$, where m_i and n_i are the mass and number density, respectively, of each species [66]. Thus, PBH relaxation is determined on the basis of the distributions of main-sequence stars (MSs) [62], virtually independent of μ.

The angular momentum relaxation time is

$$t_J(J,a) = t_h \left[\frac{J}{J_m(a)}\right]^2 \left(\frac{a}{r_h}\right)^p . \tag{13}$$

Here, a is the semimajor axis of an orbit, and $J_m(a) = \sqrt{Ma}$ is the maximal (circular) angular momentum for a specific energy. p describes the spatial profile of the MSs (i.e., $n_{\rm MS} \sim r^{-3/2-p}$).

Subsequently, we estimate the timescale of a slow inspiral. The energy carried away by gravitational radiation per period is expressed as follows [47, 63]:

$$\Delta E = E_1 \left(\frac{J}{J_{lc}}\right)^{-7} \tag{14}$$

with

$$E_1 = \frac{85\pi}{3\times 2^{13}}\frac{\mu}{M}; \quad J_{lc} = 4M. \tag{15}$$

Note that they are defined in units of μ.

For a high eccentricity orbit, periapse remains approximately a constant, and the time for a CO with initial specific energy ϵ_0 to finish the inspiral is

$$t_0 = \int_{\epsilon_0}^{\infty} \frac{d\epsilon}{d\epsilon/dt} \approx \frac{2\pi\sqrt{Ma}}{\Delta E} \sim \mu^{-1}. \tag{16}$$

Ensuring that the slow inspiral can continue without being disrupted by further scatterings is vital. A critical value of a is defined as $t_0(J_{lc}, a_c)/t_J(J_{lc}, a_c) = 1$. A CO is likely to fall into an SMBH without disruptions with $a < a_c$, where

$$\frac{a_c}{r_h} = \left(\frac{d_c}{r_h}\right)^{\frac{3}{3-2p}}; \quad d_c = \left(\frac{8\sqrt{M}E_1 t_h}{\pi}\right)^{2/3} . \tag{17}$$

The intrinsic EMRI rate for PBHs with arbitrary mass can be estimated using the analytic solution of the Fokker-Planck equation [63],

$$\begin{aligned}\mathcal{R}_{\rm PBH}(M,\mu) &\sim \frac{n_{\rm PBH}(r_h)}{t_h \ln[J_m(a_c)/J_{lc}]}\left(\frac{a_c}{r_h}\right)^{3/2-2p} \\ &\sim \mathcal{G}(M,\mu)\left(\frac{\mu}{10M_\odot}\right)^{\frac{4p-3}{2p-3}} \mathcal{R}_{\rm astro}(M)\end{aligned} \tag{18}$$

where $n_{\rm PBH}(a)$ is the PBH number density at a [82]. p ranges from 0 to 0.25, where 0 indicates a great likelihood [65, 67–69].

PBH Constraints. Finally, the SMBH mass spectrum has been given in [31, 32],

$$\frac{dn}{d\ln M} = 0.005\left(\frac{M}{3\times 10^6 M_\odot}\right)^{-0.3} {\rm Mpc}^{-3}, \tag{19}$$

with $10^4 M_\odot \le M \le 10^7 M_\odot$. The expected observable PBH-SMBH EMRI rate can be converted into the sensitivity to the PBH energy density fraction of DM, $f_{\rm PBH}$.

Immediately after observation, the information on the system can be extracted using a detailed waveform [32, 48]. In particular, μ can be measured by analyzing the orbit's time-dependence. Stellar BHs have masses from 5 to several tens of $M_\odot$ [70]. If PBHs are within the same mass regime (e.g., motivated in [71]), stellar BHs may behave as a background in PBH search processes. Similarly, neutron stars and white dwarfs may contribute to the PBH-SMBH background. The mass of white dwarfs (neutron stars) is unlikely to be inferior to 0.6 $M_\odot$ (1 $M_\odot$). If PBHs are substantially lighter than such astrophysical COs, the background is free, and the observation of one event may be sufficient for declaring discovery.

In Fig. 2, we present the value of $f_{\rm PBH}$ yielding one PBH-SMBH EMRI with an SNR of > 15 during a 5-year experiment conducted using various GW detectors. The dark gray region starts at 3 $M_\odot$ for the stellar BH background. From 0.3 $M_\odot$, white dwarfs and neutron stars become important, labeled in light gray. We stop our calculation at $\mu = 10^2 M_\odot$ so that the EMRI remains a reasonable approximation. The existing constraints on $f_{\rm PBH}$ are included. LISA-like GW experiments have favorable potential for probing the unexplored parameter space.

Several essential features of this sensitivity curve include the following:

i). When μ is not excessively small and a sufficiently sensitive GW detector is applied, all EMRIs occuring within $z = 1$ can be observed. When $p = 0$, the intrinsic EMRI rate $\mathcal{R}_{\rm PBH}(M,\mu)$ is independent of μ. This explains the flatness of the $f_{\rm PBH}$ curves in the large μ regime. When μ is lowered, not all EMRIs exceed the SNR threshold. This produces the turning point that is determined on the basis of the detector sensitivity.

ii). As discussed following Eq.(9), for a fixed μ, a smaller M yields a larger $\Delta f/f$ during the calculation of the SNR (i.e. $\Delta f/f \sim 1/M^2$). Although the GW strain scales as $h_c \sim \sqrt{M}$, a superior SNR can be achieved for lighter SMBHs assuming h_n is the same. The SMBH mass distribution also increases when M decreases, which indicates that a GW experiment may possess superior sensitivity for lighter PBHs if its optimal frequency region is higher. This explains why the reach of the DECi-Hertz Interferometer Gravitational wave Observatory (DECIGO) is comparable to that of Big Bang Observer (BBO) with inferior sensitivity in lower frequency regions.

In Fig. 2, we also present the reach limit with a different p, shown as the dashed curve for the LISA(C1). For

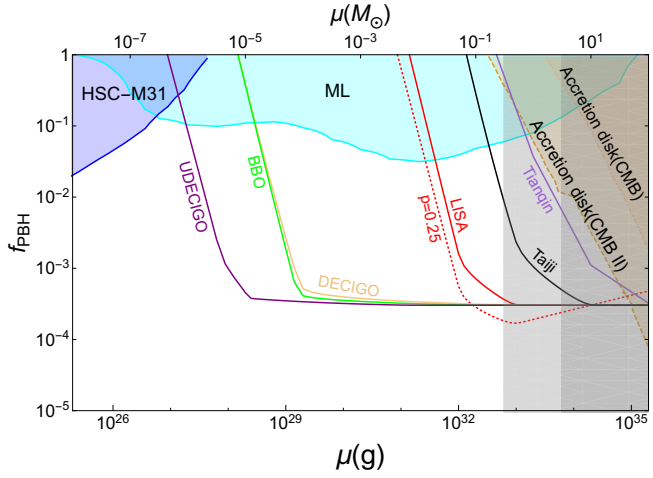

FIG. 2: The value of $f_{\rm PBH}(\mu)$ yielding one observable PBH-SMBH EMRI event during a 5-year experiment. The solid lines are for $p = 0$. The dashed red line corresponds to the LISA C1 sensitivity associated with $p = 0.25$. The microlensing constraint, HSC-M31, is from [7]. Other constraints are from [2, 72]. The regions where $0.3M_\odot < \mu < 3M_\odot$ and $3M_\odot < \mu < 100M_\odot$ are shaded for possible background from neutron stars (white dwarfs) [73, 74] and stellar BHs, respectively.

$p \neq 0$, the intrinsic EMRI rate depends non-trivially on μ. When p is positive, the reach improves for a lighter PBH. p is related to the spatial distribution of the MS that controls the relaxation time. It also affects the EMRI rate of merging SMBHs and ordinary astrophysical COs, the observation of which can help to reduce the uncertainty in our PBH-SMBH rate calculation.

Discussion. In this letter, we explore the possibility of using LISA-like GW detectors to seek PBH-SMBH EMRI events. The frequency of GWs is determined on the basis of the SMBH mass. A vast range of PBH masses can be probed. In particular, a BH much lighter than 0.3 $M_\odot$ is not expected from astrophysics. Detection of such a SMBH-PBH merger outside the astrophysical CO mass window would be particularly vital in PBH search processes.

Our analysis investigates, for the first time, a PBH-as-DM scenario by using LISA-like GW detectors, thus, connecting astronomy to GW and DM physics. The sensitivity to $f_{\rm PBH}$ in certain mass regimes may reach $10^{-3} - 10^{-4}$, substantially superior to existing sensitivity. Our results could be considerably improved with better knowledge from those interdisciplinary areas. For example, we truncate our calculation at $z = 1$ because the validity of astrophysical empirical relations, such as Eq.(5) is uncertain at high redshift. With a more thorough understanding, a higher z region could be included, and a smaller $f_{\rm PBH}$ could be explored. Furthermore, astrophysical uncertainties, such as SMBH mass and spin distributions, would affect the rate estimation. The observation of EMRI events by astrophysical COs provides valuable information and feedbacks for our PBH calculation.

As a final comment, lighter SMBHs may potentially be more valuable in the search for small-mass PBHs, because of both the higher number density from the SMBH mass spectrum and the larger integration range of frequency in the SNR calculation. This serves as a guideline for optimizing a light PBH search processes in future LISA-like GW experiments.

Acknowledgement. We thank Yanbei Chen, Runqiu Liu, Aaron Pierce, Tao Ren, Keith Riles, and Ben Safdi for their valuable discussions. In particular, we thank Xian Chen and Josh Foster for carefully reading our manuscript and providing valuable comments. JS is supported by the National Natural Science Foundation of China (NSFC) under grant No.11647601, No.11690022, and No.11675243 and is also supported by the Strategic Priority Research Program of the Chinese Academy of Sciences under grant No.XDB21010200 and No.XDB23030100. YZ is grateful for the grant awarded by the Office of Science and Technology, Shanghai Municipal Government (No. 16DZ2260200). YZ also thanks supported by the U.S. Department of Energy for their grant (No.DE-SC0007859).

I. APPENDIX

In this appendix, we provide a back-of-envelop estimation to describe the behavior of the sensitivity curve in Fig. 2.

First, for large enough PBH mass, say $10M_\odot$, all PBH-SMBH EMRIs within the cutoff radius 3.5Gpc can be detected by the GW detectors considered in this paper. Thus the number of evernts after 5-year operation can be written as

$$5\mathrm{yr} \times \int \mathrm{dM}\mathcal{G}(\mathrm{M}, 10\mathrm{M}_\odot)\mathcal{R}_{\rm astro}(\mathrm{M})\frac{\mathrm{dn}}{\mathrm{d}\ln\mathrm{M}}\frac{4\pi}{3}(3.5\mathrm{Gpc})^3 \approx 3300, \quad (20)$$

where $\mathcal{G}$ is the scale factor introduced in Eq. 12, $\mathcal{R}_{\rm astro}$ is the intrinsic EMRI rate for a single galaxy defined in Eq. 11, $dn/d\ln M$ is the SMBH mass distribution in Eq. 19 and the final factor is the volume integral. Assuming one event detection, this number translates into a limit $f_{\rm PBH} \approx 0.0003$ and corresponds to the position of the flat lines in Fig. 2.

As the PBH mass decreases, the GW signal is weakened and the maximum distance($r_{\rm max}$) with SNR ≥ 15 shrinks. When $r_{\rm max} < 3.5$Gpc, the number of events is reduced and the sensitivity curves in Fig. 2 start to turn up. The location of the turning point depends on the sensitivity of each detector. Taking LISA as an example, we can estimate roughly this location with a simplified input of the GW signals. The GW amplitudes(for the two polarizations $+, \times$) of a binary with a chirp mass M_c

are of order(see e.g., [78])

$$h_{+,\times} = \frac{4}{r}\left(\frac{GM_c}{c^2}\right)^{5/3}\left(\frac{\pi f}{c}\right)^{2/3}, \tag{21}$$

where we have switched to the SI unit by restoring the factors of G and c. The characteristic strain h_c is given roughly by [53]:

$$h_c = h_{+,\times}\sqrt{\frac{2f^2}{df/dt}}, \tag{22}$$

and df/dt is [78]:

$$\frac{df}{dt} = \frac{96c^2}{5}\pi^{8/3}\left(\frac{GM_c}{c^2}\right)^{5/3}\left(\frac{f}{c}\right)^{11/3}. \tag{23}$$

With this relatively simple amplitude input, one can easily find thecritical mass of PBH, below which $r_{\max}$ starts to become smaller than 3.5Gpc. For a generic choice of SMBH mass, $M = 10^6 M_\odot$, we find this occurs at $\mu \approx 0.03 M_\odot$ given LISA's sensitivity. This result is consistent with the turning point in Fig. 2. The similar analysis can be applied to other GW detectors.

[1] **Planck** Collaboration, P. A. R. Ade *et al.*, "Planck 2015 results. XIII. Cosmological parameters," *Astron. Astrophys.* **594** (2016) A13, arXiv:1502.01589 [astro-ph.CO].

[2] B. Carr, F. Kuhnel, and M. Sandstad, "Primordial Black Holes as Dark Matter," *Phys. Rev.* **D94** no. 8, (2016) 083504, arXiv:1607.06077 [astro-ph.CO].

[3] B. J. Carr, K. Kohri, Y. Sendouda, and J. Yokoyama, "New cosmological constraints on primordial black holes," *Phys. Rev.* **D81** (2010) 104019, arXiv:0912.5297 [astro-ph.CO].

[4] R. J. Nemiroff, G. F. Marani, J. P. Norris, and J. T. Bonnell, "Limits on the cosmological abundance of supermassive compact objects from a millilensing search in gamma-ray burst data," *Phys. Rev. Lett.* **86** (2001) 580, arXiv:astro-ph/0101488 [astro-ph].

[5] J. J. Dalcanton, C. R. Canizares, A. Granados, C. C. Steidel, and J. T. Stocke, "Observational limits on Omega in stars, brown dwarfs, and stellar remnants from gravitational microlensing," *Astrophys. J.* **424** (Apr., 1994) 550–568.

[6] P. N. Wilkinson, D. R. Henstock, I. W. A. Browne, A. G. Polatidis, P. Augusto, A. C. S. Readhead, T. J. Pearson, W. Xu, G. B. Taylor, and R. C. Vermeulen, "Limits on the cosmological abundance of supermassive compact objects from a search for multiple imaging in compact radio sources," *Phys. Rev. Lett.* **86** (2001) 584–587, arXiv:astro-ph/0101328 [astro-ph].

[7] H. Niikura *et al.*, "Microlensing constraints on primordial black holes with the Subaru/HSC Andromeda observation," arXiv:1701.02151 [astro-ph.CO].

[8] **EROS-2** Collaboration, P. Tisserand *et al.*, "Limits on the Macho Content of the Galactic Halo from the EROS-2 Survey of the Magellanic Clouds," *Astron. Astrophys.* **469** (2007) 387–404, arXiv:astro-ph/0607207 [astro-ph].

[9] L. Wyrzykowski *et al.*, "The OGLE View of Microlensing towards the Magellanic Clouds. IV. OGLE-III SMC Data and Final Conclusions on MACHOs," *Mon. Not. Roy. Astron. Soc.* **416** (2011) 2949, arXiv:1106.2925 [astro-ph.GA].

[10] **Macho** Collaboration, R. A. Allsman *et al.*, "MACHO project limits on black hole dark matter in the 1-30 solar mass range," *Astrophys. J.* **550** (2001) L169, arXiv:astro-ph/0011506 [astro-ph].

[11] **MACHO, EROS** Collaboration, C. Alcock *et al.*, "EROS and MACHO combined limits on planetary mass dark matter in the galactic halo," *Astrophys. J.* **499** (1998) L9, arXiv:astro-ph/9803082 [astro-ph].

[12] K. Griest, A. M. Cieplak, and M. J. Lehner, "Experimental Limits on Primordial Black Hole Dark Matter from the First 2 yr of Kepler Data," *Astrophys. J.* **786** no. 2, (2014) 158, arXiv:1307.5798 [astro-ph.CO].

[13] M. Ricotti, J. P. Ostriker, and K. J. Mack, "Effect of Primordial Black Holes on the Cosmic Microwave Background and Cosmological Parameter Estimates," *Astrophys. J.* **680** (2008) 829, arXiv:0709.0524 [astro-ph].

[14] L. Chen, Q.-G. Huang, and K. Wang, "Constraint on the abundance of primordial black holes in dark matter from Planck data," *JCAP* **1612** no. 12, (2016) 044, arXiv:1608.02174 [astro-ph.CO].

[15] Y. Ali-Hamoud and M. Kamionkowski, "Cosmic microwave background limits on accreting primordial black holes," *Phys. Rev.* **D95** no. 4, (2017) 043534, arXiv:1612.05644 [astro-ph.CO].

[16] A. M. Green, "Astrophysical uncertainties on stellar microlensing constraints on multi-Solar mass primordial black hole dark matter," *Phys. Rev.* **D96** no. 4, (2017) 043020, arXiv:1705.10818 [astro-ph.CO].

[17] **Virgo, LIGO Scientific** Collaboration, B. P. Abbott *et al.*, "Observation of Gravitational Waves from a Binary Black Hole Merger," *Phys. Rev. Lett.* **116** no. 6, (2016) 061102, arXiv:1602.03837 [gr-qc].

[18] **Virgo, LIGO Scientific** Collaboration, B. P. Abbott *et al.*, "GW151226: Observation of Gravitational Waves from a 22-Solar-Mass Binary Black Hole Coalescence," *Phys. Rev. Lett.* **116** no. 24, (2016) 241103, arXiv:1606.04855 [gr-qc].

[19] **VIRGO, LIGO Scientific** Collaboration, B. P. Abbott *et al.*, "GW170104: Observation of a 50-Solar-Mass Binary Black Hole Coalescence at Redshift 0.2," *Phys. Rev. Lett.* **118** no. 22, (2017) 221101, arXiv:1706.01812 [gr-qc]. [Erratum: Phys. Rev. Lett.121,no.12,129901(2018)].

[20] S. Bird, I. Cholis, J. B. Muoz, Y. Ali-Hamoud, M. Kamionkowski, E. D. Kovetz, A. Raccanelli, and A. G. Riess, "Did LIGO detect dark matter?," *Phys. Rev. Lett.* **116** no. 20, (2016) 201301, arXiv:1603.00464 [astro-ph.CO].

[21] M. Sasaki, T. Suyama, T. Tanaka, and S. Yokoyama, "Primordial Black Hole Scenario for the Gravitational-Wave Event GW150914," *Phys. Rev. Lett.* **117** no. 6, (2016) 061101, arXiv:1603.08338 [astro-ph.CO]. [erratum: Phys. Rev. Lett.121,no.5,059901(2018)].

[22] Y. N. Eroshenko, "Gravitational waves from primordial black holes collisions in binary systems," *J. Phys. Conf. Ser.* **1051** no. 1, (2018) 012010, arXiv:1604.04932 [astro-ph.CO].

[23] S. Clesse and J. Garca-Bellido, "Detecting the gravitational wave background from primordial black hole dark matter," *Phys. Dark Univ.* **18** (2017) 105–114, arXiv:1610.08479 [astro-ph.CO].

[24] N. Orlofsky, A. Pierce, and J. D. Wells, "Inflationary theory and pulsar timing investigations of primordial black holes and gravitational waves," *Phys. Rev.* **D95** no. 6, (2017) 063518, arXiv:1612.05279 [astro-ph.CO].

[25] H. Nishikawa, E. D. Kovetz, M. Kamionkowski, and J. Silk, "Primordial-black-hole mergers in dark-matter spikes," arXiv:1708.08449 [astro-ph.CO].

[26] M. Raidal, V. Vaskonen, and H. Veerme, "Gravitational Waves from Primordial Black Hole Mergers," *JCAP* **1709** (2017) 037, arXiv:1707.01480 [astro-ph.CO].

[27] Y. Ali-Hamoud, E. D. Kovetz, and M. Kamionkowski, "Merger rate of primordial black-hole binaries," *Phys. Rev.* **D96** no. 12, (2017) 123523, arXiv:1709.06576 [astro-ph.CO].

[28] Z.-C. Chen and Q.-G. Huang, "Merger Rate Distribution of Primordial-Black-Hole Binaries," *Astrophys. J.* **864** no. 1, (2018) 61, arXiv:1801.10327 [astro-ph.CO].

[29] **LISA** Collaboration, H. Audley *et al.*, "Laser Interferometer Space Antenna," arXiv:1702.00786 [astro-ph.IM].

[30] P. Amaro-Seoane, J. R. Gair, A. Pound, S. A. Hughes, and C. F. Sopuerta, "Research Update on Extreme-Mass-Ratio Inspirals," *J. Phys. Conf. Ser.* **610** no. 1, (2015) 012002, arXiv:1410.0958 [astro-ph.CO].

[31] A. Klein *et al.*, "Science with the space-based interferometer eLISA: Supermassive black hole binaries," *Phys. Rev.* **D93** no. 2, (2016) 024003, arXiv:1511.05581 [gr-qc].

[32] S. Babak, J. Gair, A. Sesana, E. Barausse, C. F. Sopuerta, C. P. L. Berry, E. Berti, P. Amaro-Seoane, A. Petiteau, and A. Klein, "Science with the space-based interferometer LISA. V: Extreme mass-ratio inspirals," *Phys. Rev.* **D95** no. 10, (2017) 103012, arXiv:1703.09722 [gr-qc].

[33] P. J. E. Peebles, "Star Distribution Near a Collapsed Object," *Astrophys. J.* **178** (Dec., 1972) 371–376.

[34] L. Ferrarese and D. Merritt, "A Fundamental relation between supermassive black holes and their host galaxies," *Astrophys. J.* **539** (2000) L9, arXiv:astro-ph/0006053 [astro-ph].

[35] K. Gebhardt *et al.*, "A Relationship between nuclear black hole mass and galaxy velocity dispersion," *Astrophys. J.* **539** (2000) L13, arXiv:astro-ph/0006289 [astro-ph].

[36] S. Tremaine *et al.*, "The slope of the black hole mass versus velocity dispersion correlation," *Astrophys. J.* **574** (2002) 740–753, arXiv:astro-ph/0203468 [astro-ph].

[37] J. Dubinski and R. G. Carlberg, "The Structure of cold dark matter halos," *Astrophys. J.* **378** (1991) 496.

[38] J. F. Navarro, C. S. Frenk, and S. D. M. White, "The Structure of cold dark matter halos," *Astrophys. J.* **462** (1996) 563–575, arXiv:astro-ph/9508025 [astro-ph].

[39] J. F. Navarro, C. S. Frenk, and S. D. M. White, "A Universal density profile from hierarchical clustering," *Astrophys. J.* **490** (1997) 493–508, arXiv:astro-ph/9611107 [astro-ph].

[40] B. Moore, T. R. Quinn, F. Governato, J. Stadel, and G. Lake, "Cold collapse and the core catastrophe," *Mon. Not. Roy. Astron. Soc.* **310** (1999) 1147–1152, arXiv:astro-ph/9903164 [astro-ph].

[41] S. Tulin and H.-B. Yu, "Dark Matter Self-interactions and Small Scale Structure," *Phys. Rept.* **730** (2018) 1–57, arXiv:1705.02358 [hep-ph].

[42] P. Gondolo and J. Silk, "Dark matter annihilation at the galactic center," *Phys. Rev. Lett.* **83** (1999) 1719–1722, arXiv:astro-ph/9906391 [astro-ph].

[43] L. Sadeghian, F. Ferrer, and C. M. Will, "Dark matter distributions around massive black holes: A general relativistic analysis," *Phys. Rev.* **D88** no. 6, (2013) 063522, arXiv:1305.2619 [astro-ph.GA].

[44] F. Ferrer, A. M. da Rosa, and C. M. Will, "Dark matter spikes in the vicinity of Kerr black holes," *Phys. Rev.* **D96** no. 8, (2017) 083014, arXiv:1707.06302 [astro-ph.CO].

[45] A. A. Dutton and A. V. Macci, "Cold dark matter haloes in the Planck era: evolution of structural parameters for Einasto and NFW profiles," *Mon. Not. Roy. Astron. Soc.* **441** no. 4, (2014) 3359–3374, arXiv:1402.7073 [astro-ph.CO].

[46] L. Ferrarese, "Beyond the bulge: a fundamental relation between supermassive black holes and dark matter halos," *Astrophys. J.* **578** (2002) 90–97, arXiv:astro-ph/0203469 [astro-ph].

[47] P. C. Peters and J. Mathews, "Gravitational radiation from point masses in a Keplerian orbit," *Phys. Rev.* **131** (1963) 435–439.

[48] L. Barack and C. Cutler, "LISA capture sources: Approximate waveforms, signal-to-noise ratios, and parameter estimation accuracy," *Phys. Rev.* **D69** (2004) 082005, arXiv:gr-qc/0310125 [gr-qc].

[49] J. R. Gair and K. Glampedakis, "Improved approximate inspirals of test-bodies into Kerr black holes," *Phys. Rev.* **D73** (2006) 064037, arXiv:gr-qc/0510129 [gr-qc].

[50] S. Babak, H. Fang, J. R. Gair, K. Glampedakis, and S. A. Hughes, "'Kludge' gravitational waveforms for a test-body orbiting a Kerr black hole," *Phys. Rev.* **D75** (2007) 024005, arXiv:gr-qc/0607007 [gr-qc]. [Erratum: Phys. Rev.D77,04990(2008)].

[51] S. A. Teukolsky, "Perturbations of a rotating black hole. 1. Fundamental equations for gravitational electromagnetic and neutrino field perturbations," *Astrophys. J.* **185** (1973) 635–647.

[52] M. Sasaki and T. Nakamura, "Gravitational Radiation From a Kerr Black Hole. 1. Formulation and a Method for Numerical Analysis," *Prog. Theor. Phys.* **67** (1982) 1788.

[53] L. S. Finn and K. S. Thorne, "Gravitational waves from a compact star in a circular, inspiral orbit, in the equatorial plane of a massive, spinning black hole, as observed by LISA," *Phys. Rev.* **D62** (2000) 124021,

arXiv:gr-qc/0007074 [gr-qc].

[54] J. R. Gair, "Probing black holes at low redshift using LISA EMRI observations," *Class. Quant. Grav.* **26** (2009) 094034, arXiv:0811.0188 [gr-qc].

[55] J. M. Bardeen, W. H. Press, and S. A. Teukolsky, "Rotating black holes: Locally nonrotating frames, energy extraction, and scalar synchrotron radiation," *Astrophys. J.* **178** (1972) 347.

[56] C. J. Moore, R. H. Cole, and C. P. L. Berry, "Gravitational-wave sensitivity curves," *Class. Quant. Grav.* **32** no. 1, (2015) 015014, arXiv:1408.0740 [gr-qc].

[57] C. Caprini *et al.*, "Science with the space-based interferometer eLISA. II: Gravitational waves from cosmological phase transitions," *JCAP* **1604** no. 04, (2016) 001, arXiv:1512.06239 [astro-ph.CO].

[58] X. Gong *et al.*, "Descope of the ALIA mission," *J. Phys. Conf. Ser.* **610** no. 1, (2015) 012011, arXiv:1410.7296 [gr-qc].

[59] **TianQin** Collaboration, J. Luo *et al.*, "TianQin: a space-borne gravitational wave detector," *Class. Quant. Grav.* **33** no. 3, (2016) 035010, arXiv:1512.02076 [astro-ph.IM].

[60] H. Kudoh, A. Taruya, T. Hiramatsu, and Y. Himemoto, "Detecting a gravitational-wave background with next-generation space interferometers," *Phys. Rev.* **D73** (2006) 064006, arXiv:gr-qc/0511145 [gr-qc].

[61] C. W. Misner, K. S. Thorne, and J. A. Wheeler, *Gravitation*. W. H. Freeman, San Francisco, 1973.

[62] C. Hopman, "Extreme mass ratio inspiral rates: dependence on the massive black hole mass," *Class. Quant. Grav.* **26** (2009) 094028, arXiv:0901.1667 [astro-ph].

[63] C. Hopman and T. Alexander, "The Orbital statistics of stellar inspiral and relaxation near a massive black hole: Characterizing gravitational wave sources," *Astrophys. J.* **629** (2005) 362–372, arXiv:astro-ph/0503672 [astro-ph].

[64] C. Hopman and T. Alexander, "Resonant relaxation near a massive black hole: the stellar distribution and gravitational wave sources," *Astrophys. J.* **645** (2006) 1152–1163, arXiv:astro-ph/0601161 [astro-ph].

[65] C. Hopman and T. Alexander, "The effect of mass-segregation on gravitational wave sources near massive black holes," *Astrophys. J.* **645** (2006) L133–L136, arXiv:astro-ph/0603324 [astro-ph].

[66] J. Miralda-Escude and A. Gould, "A cluster of black holes at the galactic center," *Astrophys. J.* **545** (2000) 847, arXiv:astro-ph/0003269 [astro-ph].

[67] P. Amaro-Seoane and M. Preto, "The impact of realistic models of mass segregation on the event rate of extreme-mass ratio inspirals and cusp re-growth," *Class. Quant. Grav.* **28** (2011) 094017, arXiv:1010.5781 [astro-ph.CO].

[68] T. Alexander and C. Hopman, "Strong mass segregation around a massive black hole," *Astrophys. J.* **697** (2009) 1861–1869, arXiv:0808.3150 [astro-ph].

[69] M. Preto and P. Amaro-Seoane, "On strong mass segregation around a massive black hole: Implications for lower-frequency gravitational-wave astrophysics," *Astrophys. J.* **708** (2010) L42, arXiv:0910.3206 [astro-ph.GA].

[70] K. Belczynski, T. Bulik, C. L. Fryer, A. Ruiter, J. S. Vink, and J. R. Hurley, "On The Maximum Mass of Stellar Black Holes," *Astrophys. J.* **714** (2010) 1217–1226, arXiv:0904.2784 [astro-ph.SR].

[71] J. Georg and S. Watson, "A Preferred Mass Range for Primordial Black Hole Formation and Black Holes as Dark Matter Revisited," *JHEP* **09** (2017) 138, arXiv:1703.04825 [astro-ph.CO]. [JHEP09,138(2017)].

[72] M. Sasaki, T. Suyama, T. Tanaka, and S. Yokoyama, "Primordial black holesperspectives in gravitational wave astronomy," *Class. Quant. Grav.* **35** no. 6, (2018) 063001, arXiv:1801.05235 [astro-ph.CO].

[73] B. Kiziltan, A. Kottas, M. De Yoreo, and S. E. Thorsett, "The Neutron Star Mass Distribution," *Astrophys. J.* **778** (2013) 66, arXiv:1309.6635 [astro-ph.SR].

[74] S. O. Kepler, D. Koester, A. D. Romero, G. Ourique, and I. Pelisoli, "White Dwarf Mass Distribution," in *20th European White Dwarf Workshop*, P.-E. Tremblay, B. Gaensicke, and T. Marsh, eds., vol. 509 of *Astronomical Society of the Pacific Conference Series*, p. 421. Mar., 2017. arXiv:1610.00371 [astro-ph.SR].

[75] V. Takhistov, "Transmuted Gravity Wave Signals from Primordial Black Holes," *Phys. Lett.* **B782** (2018) 77–82, arXiv:1707.05849 [astro-ph.CO].

[76] F. Khnel, G. D. Starkman, and K. Freese, "Primordial Black-Hole and Macroscopic Dark-Matter Constraints with LISA," arXiv:1705.10361 [gr-qc].

[77] D. Merritt, "Evolution of the dark matter distribution at the galactic center," *Phys. Rev. Lett.* **92** (2004) 201304, arXiv:astro-ph/0311594 [astro-ph].

[78] S. Husa, "Michele Maggiore: Gravitational waves. Volume 1: Theory and experiments," *Gen. Rel. Grav.* **41** (2009) 1667–1669.

[79] Transmuted gravity wave signals from extremely small mass PBH are studied in [75].

[80] The BBO and DECIGO data are taken from the website http://rhcole.com/apps/GWplotter/

[81] Using LISA to detect the stochastic GW radiation produced by PBHs orbiting Sagittarius A* is discussed in [76]. However, as we discuss later, PBH-COs scatterings are crucial for counting events. Neglecting them will result in a excessively overestimated signal. Furthermore, the GW frequency spans a large range. Careful study is necessary to properly calculate SNR.

[82] In Eq.(18) we assume that the spatial distribution of PBH and MS share the same p in the power law $(n_{\rm PBH}(r) \sim n_{\rm PBH}(r_h)(r/r_h)^{-3/2-p})$. According to Ref. [77], for light PBHs $\mu \leq \mathcal{O}(1)\ M_\odot$, this is reasonable.